Particle foraging strategies promote microbial diversity in marine environments

Authors: Ali Ebrahimi[1†], Akshit Goyal[2†], Otto X. Cordero[1*]

Authors affiliation:

[1] *Ralph M. Parsons Laboratory for Environmental Science and Engineering, Department of Civil and Environmental Engineering, Massachusetts Institute of Technology, Cambridge, MA 02139 USA*

[2] *Physics of Living Systems, Department of Physics, Massachusetts Institute of Technology, Cambridge, MA 02139, USA*

* Correspondence to: ottox@mit.edu

† Equal contribution.

Abstract:

Microbial foraging in patchy environments, where resources are fragmented into particles or pockets embedded in a large matrix, plays a key role in natural environments. In the oceans and freshwater systems, particle-associated bacteria can interact with particle surfaces in different ways: some colonize only during short transients, while others form long-lived, stable colonies. We do not yet understand the ecological mechanisms by which both short-term and long-term colonizers can coexist. Here, we address this problem with a mathematical model that explains how marine populations with different detachment rates from particles can stably coexist. In our model, populations grow only while on particles, but also face the increased risk of mortality by predation and sinking. Key to coexistence is the idea that detachment from particles modulates both net growth and mortality, but in opposite directions, creating a trade-off between them. While slow-detaching populations show the highest growth return (i.e., produce more net offspring), they are more susceptible to suffer higher rates of mortality than fast-detaching populations. Surprisingly, fluctuating environments, manifesting as blooms of particles (favoring growth) and predators (favoring mortality) significantly expand the likelihood that populations with different detachment rates can coexist. Our study shows how the spatial ecology of microbes in the ocean can lead to a predictable diversification of foraging strategies and the coexistence of multiple taxa on a single growth-limiting resource.

Introduction

Microbes in nature are remarkably diverse, with thousands of species coexisting in any few milliliters of seawater or grains of soils [1,2]. This extreme diversity is puzzling since it conflicts with classic ecological predictions. This puzzle has classically been termed "the paradox of the plankton," referring to the discrepancy between the measured diversity of planktons in the ocean, and the diversity expected based on the number of limiting nutrients[3–6]. Decades of work have helped, in part, to provide solutions for this paradox in the context of free-living (i.e., planktonic) microbes in the ocean. Many have suggested new sources of diversity, such as spatiotemporal variability, microbial interactions, and grazing[7–9]. However, in contrast with free-living microbes, the diversity of particle-associated microbes — often an order of magnitude greater than free-living ones — has been overlooked[10–12]. In contrast with planktonic bacteria, which float freely in the ocean and consume nutrients from dissolved organic matter, particle-associated microbes grow by attaching to and consuming small fragments of particulate organic matter (of the order of micrometers to millimeters). It is thus instructive to ask: what factors contribute to the observed diversity of particle-associated microbes, and how do these factors collectively influence the coexistence of particle-associated microbes?

The dispersal strategies of particle-associated microbes can be effectively condensed into one parameter: the rate at which they detach from particles. This rate, which is the inverse of the average time that microbes spend on a particle, is the key trait distinguishing particle-associated microbial populations from planktonic ones[13,14]The detachment rates of such particle-associated taxa can be quite variable[15,16]. Bacteria with low detachment rates form biofilms on particles for efficient exploitation of the resources locally, while others with high detachment rates frequently attach and detach across many different particles to access new resources[17]. Therefore, to understand how diversity is maintained in particle-associated bacteria we must be able to explain how bacteria with different dispersal rates can coexist. In this study, we address this question. Specifically, we ask how two populations with different dispersal strategies can coexist while competing for the same set of particles. We address this question under a range of conditions relevant for marine microbes.

We hypothesize that dispersal is key to the coexistence of particle-associated microbes and thus might explain their high diversity. The degree of species coexistence on particles depends on the balance between growth and mortality. On particles, net mortality rates can be higher

than for planktonic cells because of the large congregation of cells on particles, which exposes them to the possibility of a large and sudden local population collapse. The collapse of a particle-attached population can be induced by a variety of mechanisms, including particles sinking below a habitable zone[18], or predation of whole bacterial colonies by viruses or grazers . For instance, after a lytic phage bursts out of a few cells on a particle, virions can rapidly engulf the entire bacterial population, leading to its local demise[11,19,20]. Such particle-wide mortality may kill more than 30% of particle associated populations in the ocean[21,22]. The longer a population stays on a particle, the higher the chance it will be wiped out. This trade-off between growth and risk of mortality suggests that there could be an optimal residence time on particles. It is however unclear whether such a trade-off could enable the coexistence of populations with different dispersal strategies and, if so, under what conditions.

Here we study this trade-off using mathematical models and stochastic simulations. These models reveal that the trade-off between growth and survival against predation can indeed lead to the stable coexistence of particle-associated microbial populations with different dispersal strategies (in our work, detachment rates). We also study how environmental parameters, such as the supply rate of new particles, determine the dominant dispersal strategy and the range of stable coexistence. Our results show that in bloom conditions, when the particle supply is high, fast dispersers that rapidly hop between particles are favored. In contrast, under oligotrophic conditions, when particles are rare, rarely detaching bacteria have a competitive advantage. Overall, our work shows that differences in dispersal strategies alone can enable the coexistence of particle-associated marine bacteria, in part explaining their impressive natural diversity.

Results

Overview of the model: To understand how differences in dispersal strategies affect bacterial coexistence, we developed a mathematical model that describes the population dynamics of bacteria colonizing a bath of particles with a chosen dispersal strategy. More specifically, in our model, bacterial cells attach to particles from a free-living population in the bulk of the bath; they then grow and reproduce while attached. Detachment is stochastic with a fixed rate. After detachment, cells re-enter the free-living population and repeat the process. During the time spent attached to particles, all bacteria on a particle may die with a fixed probability per unit time, corresponding to their particle-wide mortality rate (Figure 1A). Another important feature of

the model is density-dependent growth, which means that per capita growth rates decrease with increasing population size. For this, we use the classic logistic growth equation, which contains a simple linear density dependence (Figure 1B; Methods). Free-living subpopulations cannot grow, but die at a fixed mortality rate due to starvation. The probability of a bacterium encountering particles controls bacterial attachment, which we calculate using random walk theory as the hitting probability of two objects with defined sizes[23,24] (see Methods for details). We assume that the detachment rate is an intrinsic property of a bacterial population and comprises its dispersal strategy independent of the abiotic environment. In our simulations, it is the only trait that varies between different bacterial populations. Growing evidence has shown that bacterial detachment rates differ significantly across marine bacterial communities from solely planktonic cells to biofilm-forming cells on particles[16,17]. Using this mathematical model, we asked how variation in detachment rate affects bacterial growth dynamics and the ability of multiple subpopulations to coexist on particles. For this, we simulated bacterial population dynamics on a bath of several particles and measured each population's relative abundance at a steady state (example in Figure 1C).

Bacterial mortality determines optimal foraging strategies: Our model simulates growth, competition, and dispersal in a patchy landscape, similar to classical models of resource foraging, with the additional element of mortality, both within and outside patches (i.e., particles). We hypothesized that the inclusion of mortality could play an important role in affecting the success of a dispersal strategy (i.e., detachment rate), since it would alter the cost of staying on a particle. To investigate how mortality affects dispersal strategies, we studied its effect on the optimal strategy, which forms the focus of many classical models of foraging. According to optimal foraging theory (OFT), the optimal time spent on a particle is one that balances the time spent without food while searching for a new patch, with the diminishing returns from staying on a continuously depleting patch[13,25]. In our model, particles are analogous to resource patches, and the detachment rate is simply the inverse of the time spent on a particle (residence time). We assumed that the optimal strategy maximizes the total biomass yield of the population.

As expected, OFT predicts the optimal detachment rate given a distribution of resources and search times, but only in the absence of mortality (Figure 2A). To test if our model agrees with the predictions of OFT, we calculated the optimal detachment rate (d_{opt}) using simulations of our model in the absence of mortality and compared it with OFT predictions (Methods). We found

that the optimal detachment rate, which outcompetes all other detachment rates, was consistent with OFT predictions across a wide range of particle numbers in our system (Figure 2A). Strikingly, in the presence of mortality, the optimal detachment rate (d_{opt}) changed significantly, either increasing or decreasing depending on the type of mortality. When mortality was particle-wide, the optimal detachment rate was much higher than predicted by OFT, often resulting in residence times that were many days shorter than the OFT prediction (Figure 2A). This is because it is more beneficial to detach faster when there is a higher risk of particle-wide extinction. In contrast, when mortality was only present in free-living populations (affecting individuals, not particles, at a constant per capita rate), the optimal detachment rate was much lower than predicted by OFT (Figure 2A). These results expand on our knowledge of OFT and explain that the source and strength of mortality – on individuals or on whole particles – can differently impact the optimal detachment rate.

A trade-off between growth and mortality enables the coexistence of dispersal strategies: Having observed that mortality can greatly affect the success of a dispersal strategy, we next sought to understand whether it could enable the coexistence of bacterial populations with different strategies (detachment rates). Simulations where we competed a pair of bacterial populations with different detachment rates revealed that differences in detachment rates alone are sufficient to enable coexistence on particles (Figure 2B). We assessed coexistence by measuring the relative abundances of populations at equilibrium (Figure 2 – Figure supplement 1). Interestingly, such a non-trivial coexistence only emerged in the presence of particle-wide mortality. In the absence of mortality on particles, we only observed trivial coexistence (coexisting populations had identical detachment rates, and for the purposes of the model, were one and the same; Figure 2 – Figure supplement 2). These results suggested that the presence of particle-wide mortality, where the entire population on a particle suffers rapid death, was crucial for populations with different dispersal strategies to coexist.

To investigate the underlying mechanisms that may give rise to the coexistence of populations with different detachment rates, we quantified the growth return of particle-associated populations as well as their survival rate on particles (Figure 3A-3B). We calculated the average growth return based on the average number of offspring produced per capita during one single attachment-detachment event. The survival rate on particles was obtained by subtracting the mortality rate per capita from the offspring production rate per capita (Figure 3B; see Methods). The results revealed that a trade-off between bacterial growth return and survival rate emerged

on particles, supporting the coexistence of populations with different detachment rates (Figure 3C-D). Populations that detach slowly from particles have higher growth returns but are also more susceptible to particle-associated mortality. In contrast, populations with low residence time on particles (high detachment rate) have low growth returns but they are less likely to die by predation or sink beyond the habitable zone. We next investigated whether such a trade-off was necessary to enable coexistence in our model.

We developed a coarse-grained model to address the conditions under which we might observe coexistence between populations whose only intrinsic difference was their detachment rates in our system. Our simple model expands on classical literature which describes coexistence among various dispersal strategies in spatially structured habitats[26–29]. We simplified many details in favor of analytical tractability. Chiefly, we assumed that the growth dynamics on each particle were much faster than the dispersal dynamics across particles. This allowed us to replace detailed growth dynamics on single particles with a single number quantifying the bacterial population, N, after growth on each particle. In the model, we considered two particle associated populations that competed for a shared pool of particles. To keep track of populations, we quantified the number of particles they had successfully colonized as B_1 and B_2, respectively. Individuals from both populations could detach from particles they had already colonized and migrate to a number E of yet-unoccupied particles, with a rate proportional to their detachment rates, d_1 and d_2, respectively. Once migrated, individuals rapidly grew on unoccupied particles to their fixed per particle growth returns, N_1 and N_2. To model particle-wide mortality, we assumed a fixed per particle mortality rate, m_p. The population dynamics for the system of particles could therefore be written as follows:

$$\frac{dB_i}{\partial t} = N_i d_i B_i E - m_p B_i \qquad (1)$$

At equilibrium ($\frac{\partial B_i}{\partial t} = 0 \; \forall \; i$), either population can survive in the system if and only if its net colonization and mortality rates are equal ($N_i d_i E \approx m_p$). Consequently, the product of the growth return per particle and the detachment rate of either population should be equal ($N_1 d_1 \approx N_2 d_2$). By simplifying Eq. 1 at equilibrium, this model predicts that for two competing populations to coexist, their growth returns and detachment rates on particles must follow the relation:

$$\frac{N_1}{N_2} = \frac{d_2}{d_1} \qquad (2)$$

This relationship shows that coexistence demands a trade-off between the growth return (*N*) of a bacterial population, and its detachment rate (*d*), i.e., the inverse of an individual's residence time on a particle. In other words, coexistence only emerges when the growth returns increase with the residence time on the particle ($\frac{N_1}{N_2} \sim \frac{T_1}{T_2}$). In agreement with this, simulations from our detailed model revealed that coexistence between two populations with different detachment rates only occurred in conditions where the two populations obeyed such a relationship, or trade-off (Figure 3C, grey region). We obtain the same relationship in Eq. 2 through an alternate calculation, where the relative abundances of both populations remains fixed, while the particle number varies.

While the trade-off in Eq. 2 allows coexistence and is necessary condition for it, it does not hold across all parameter values, and does not allow any pair of detachment rates to coexist (Figure 3C, white region). In particular, no detachment rate can coexist with the optimal detachment rate, thus rendering coexistence between any other set of detachment rates susceptible to invasion by this optimal strategy. Other strategies, when paired with the optimal strategy, disobey the condition in Eq. 2, and thus cannot coexist with it. Therefore, if detachment rates were allowed to evolve, only one population would survive in the long run – the one with the optimal detachment rate (Figure 2 – Figure supplement 3). Motivated by this observation, we next asked whether environmental fluctuations would render coexistence evolutionarily stable, or whether they would further destabilize the coexistence of populations with non-optimal dispersal strategies.

Environmental fluctuations stabilize and enhance the diversity of dispersal strategies:

The existence of a unique optimal strategy, even in the presence of particle-wide mortality (Figure 2A), suggests that the coexistence that we observed between populations with different detachment rates (Figure 2B) may not be evolutionarily stable. However, in the oceans, both the abundance of particles and the density of predators (such as phage) exhibit temporal and spatial fluctuations[30–32], in turn affecting the foraging dynamics of particle-associated bacterial populations. We used our model to study how the particle-wide mortality rate affects the likelihood of two particle-associated bacterial populations to coexist (see Methods). Surprisingly,

we found a negative correlation between the mortality rate and particle abundance that enhances the range of coexistence among different detachment rates (Figure 4A). At low mortality rates, slow detaching populations outcompete faster ones, as it is more advantageous to stay longer on particles and grow, i.e., these populations derive higher net growth returns. However, a higher mortality rate on particles allows faster-detaching populations to instead gain an advantage over the slow-detaching populations, since they can better avoid particle-wide mortality events.

We extended our model to ask how variation in the total number of particles (or particle abundance) affect population dynamics and the coexistence range of populations with different dispersal strategies. The results indicated that an intermediate number of particles maximize the likelihood of coexistence of two populations with different dispersal strategies (Figure 4A). Here, we simulated a range of particle abundances, between 1 to 80 particles L^{-1}, which corresponds to the commonly observed range of particle abundances in aquatic environments (mean ~25 particles L^{-1}; Figure 4 – Figure supplement 1). Low particle abundances (0 to 20 L^{-1}) promote the growth of slow detaching populations while at high particle abundances, fast detaching populations dominate. The reason for this is the following: at particle abundances less than 20 L^{-1}, the probability of free-living cells finding and attaching to particles is less than 50% of the probability at high particle abundances (100 L^{-1} in Figure 1 – Figure supplement 1). This makes particle search times very high, thus explaining how slow detaching strategies have an advantage. As the number of particles increases, the entire system can support more cells (has a higher carrying capacity). This drives a decrease in particle search times, and thus increasingly advantages faster detaching strategies.

Interestingly, our results indicate that the optimal detachment rate (d_{opt}) is affected by the particle abundance and increases with the number of particles in the system (Figure 4B). We thus hypothesized that fluctuations in particle abundance may also induce fluctuations in the optimal detachment rate, such that no specific detachment rate would be uniquely favored at all times. Thus, environmental stochasticity would constantly change the optimal detachment rate; low particle abundances would favor fast-detaching populations, while higher particle abundances would favor slow-detaching populations. Such a “fluctuating optimum” may create temporal niches and promote higher bacterial diversity on marine particles. To test this hypothesis using our model, we simulated competition between 100 populations with different detachment rates under a periodically varying particle abundance (Figure 4C). The chosen

frequencies of variation in particle abundance (F_p) were selected to be consistent with the observed frequencies in the ocean, with periods ranging between 10 to 100 hr (Figure 4 – Figure supplement 2)[33]. We quantified the range of detachment rates, a proxy for bacterial diversity, that could coexist at equilibrium (Figure 4D). The results revealed that the scenario with fastest fluctuations in particle numbers (F_p = 10hr^{-1}) supported higher diversity among populations with different detachment rates (Figure 4D). Consistent with the fluctuation periods observed in the ocean, our simulations showed that fluctuation at the daily scale is sufficient to support the coexistence of different dispersal strategies. Overall, our model provides a framework to study how environmental fluctuations contribute to observed diversity in the dispersal strategies of particle-associated populations in marine environments.

Discussion

In this study, we have shown a mechanism by which diverse dispersal strategies can coexist among bacterial populations that colonize and degrade particulate organic matter (POM) in marine environments using a mathematical model. In our model, coexistence among populations with different dispersal strategies emerges from a trade-off between growth return and the probability of survival on particles. Such a trade-off determines the net number of detaching cells from particles that disperse into the bulk environment and colonize new particles. While slow detaching populations are able to increase their growth return on particles and produce a relatively high number of offspring, they also experience higher mortality on particles that reduces their ability to colonize new particles. In contrast, faster-detaching populations can better avoid mortality by spending less time on particles, but this comes at the expense of lowering their growth return on a particle. Such populations can instead disperse and colonize a larger fraction of fresh yet-unoccupied particles. Interestingly, our results indicated that in the absence of mortality on particles, no coexistence is expected and there is a single dispersal strategy that provides the highest fitness advantage over dispersing populations, indicating that mortality on a particle is a key factor for the emergence of diverse dispersal strategies. Such correlated mortality with dispersal is the direct result of spatial structures created by particle-associated lifestyle, unlike the planktonic phase where predation probability per capita is expected to be uniform among planktonic cells. This study expands on the existing knowledge that spatial structure plays a critical role in promoting bacterial diversity in nature[34–36], by incorporating the idea of particle-wide predation, which are events of correlated predation of an entire population on a particle. Such correlated predation could be an

ecologically relevant mechanism that explains, in part, why we observe a higher diversity in particle-associated bacteria than planktonic bacteria in nature[10–12]. Our model assumes a general form of predation on particles that is insensitive to population type. However in the context of viral infection, field observations often show high strain specificity[37–40] that is likely to contribute to higher diversity in particle-associated populations. Viral infection act as a driving force to create a continuous succession of bacterial populations on particles by replacing phage exposed populations with less susceptible ones.

Consistent with the literature on optimal foraging theory[14,41,42], our model predicts the existence of an optimal foraging strategy for bacterial population colonizing particles in marine environments. Building on previous studies[13] that show the optimal detachment rate is a function of search time for new resources, our study suggests that optimal detachment rate could be significantly impacted by the predation rate on particles. Our results indicated that a high mortality rate on particles shifts the optimal foraging strategy to populations with fast detachment rates. This finding agrees with previous OFT models that considered mortality, showing that optimal foraging effort and residence time on patches decrease significantly as the density of predators increase[43,44]. Interestingly, we showed that the variability in optimal detachment rate due to environmental fluctuations in particle number and predation rate, could lead to evolutionarily stable coexistence among diverse dispersal strategies. Our results indicate that in the absence of any environmental fluctuations, there is a unique optimal dispersal strategy. However, the optimal dispersal strategy depends on the abundance of particles, and thus fluctuations in their abundance at ecological timescales could sustain multiple dispersal strategies for long times. This finding is consistent with previous theoretical and empirical studies showing that environmental fluctuations such as light and temperature may lead to the stable coexistence of species[45–48]. Our model also predicts a loss of diversity when particle abundances significantly increase, consistent with field observations from algal blooms[49–51].

While we simplified bacterial colonization dynamics on particles by only considering competitive growth kinetics, variants of our model suggest that coexistence between different dispersal strategies is also expected under more complex microbial interactions that are observed on marine particles, including cooperative growth dynamics (Figure 2 – Figure supplement 4). Such simplifications allowed us to explore the role of dispersal in maintaining microbial diversity in natural systems, in addition to previously observed factors such as metabolic interaction,

resource heterogeneities and succession[8,52,53]. However, future studies, which can build on our model, could study how additional ecological factors contribute to bacterial marine diversity, such as complex trophic interactions leading to successional dynamics [18,52,54,55]. Additionally, while we assumed diffusional searching for simplicity, extensions of our work could include more realistic bacterial search strategies, such as active motility and chemotaxis, which can play a big role in foraging in aquatic microorganisms[56–58]. Finally, though we assumed a fixed detachment rate for each population, dispersal strategies can be quite complex, depending on local conditions such as bacterial and nutrient density on particles; a more thorough exploration of the relative costs and benefits of such myriad of dispersal strategies remains another promising avenue for future work. Overall, our model provides a reliable framework to further study how diverse dispersal strategies and mortality could contribute to the emergence of complex community dynamics on marine particles and how environmental factors impact microbial processes in regulating POM turnover at the ecosystem level.

Methods

In this study, a population-based model is developed that represents the interactions between the bacterial cells with different detachment rates and particles in a chemostat system, where the total number of particles is kept constant. The following provides a detailed procedure of the modeling steps as represented schematically in Figure 1. We have made the simulation code available in the following GitHub repository: https://github.com/alieb-mit-edu/Bacterial-dispersal-model

Modeling Population Dynamics on Particles

Our model simulates the dynamics of two competing particle-associated populations (B_p) that colonize the same set of particles. Two populations (i and j) are assumed to be identical, except for their detachment rates, d, from a particle ($d_i \neq d_j$). The dynamics of the particle-associated populations are determined by the rate at which cells attach to particles (α) from the free-living population (B_F), the growth rate of attached cells (μ) and detachment rate (d), as follows:

$$\frac{dB_{p,n,i}}{\partial t} = \alpha_i B_{Fi} + \mu_i(B_{p,n})B_{p,n,i} - d_i B_{p,n,i} \qquad (3)$$

where n represents the particle index and its associated population, i. Eq. 3 can be formulated for any other population at the same particle. In a system with N_p particles and *M* populations, we numerically solve a finite set of equations (N_p × *M*) at each time interval. The growth rate of population, i (μ_i) is a function of total particle associated cells ($B_{p,n}$), as described later in Eq. 6.

From number conservation, the free-living bacterial pool B_{Fi} of any population i results from particle detachment and attachment dynamics. The rate of change of all free-living pools results from a combination of three factors: (1) the rate at which cells detach from the particles d_i, (2) the rate α_i at which cells attach to the particles, and (3) a mortality rate due to starvation m_{Fi}, as:

$$\frac{dB_{Fi}}{\partial t} = \sum_{n=1}^{N_p} d_i B_{p,n,i} - N_p \alpha_i B_{Fi} - m_{Fi} B_{Fi} \quad (4)$$

We run all dynamical simulations until an equilibrium is reached and there are no noticeable changes in the population size of particle-associated and free-living cells, i.e., $\frac{\partial B_p}{\partial t} \sim 0$ and $\frac{\partial B_F}{\partial t} \sim 0$.

Bacteria-particle encounter rate

We assume that a bacterial cell can attach to the particle it encounters and stay attached for a period of time ("residence time"). The encounter probability of a spherical cell with radius r_c and a spherical particle with a radius of r_p at a given time t can be calculated using the hitting probability from random walk theory[23,24]:

$$P_e(i) = \frac{R}{r_{c,p}} erfc\left(\frac{r_{c,p}-R}{\sqrt{4D.t}}\right) \quad (5)$$

where *R* is the total radius ($R = r_p + r_c$) and *D* is an effective diffusion coefficient ($D = D_c + D_p$) for a bacterial cell (*c*) starting at a distance ($r_{c,p}$). The diffusion coefficient can be calculated from an empirical model: $D = k_B T / 6\pi\mu r$, where $k_B \approx 1.38 \times 10^{-23}\, J\, K^{-1}$ is Boltzmann's constant, T=293 K is the ambient temperature, $\mu = 1.003\, mPa\, s$ is the viscosity of water at the given ambient temperature. In aquatic environments, the size of marine snow (>100 μm) is often a lot larger than the cell size, we thus assume that the effective diffusion is generally controlled by cell diffusion coefficient ($D \approx D_c$). From Eq. 5, we calculate the total number attaching cells to a

particle at a given time (*t*) from free living cells of population *i* by multiplying the hitting probability to the total number of free-living cells.

Growth and reproduction on particles

We assume that per capita access to particulate resources decreases in proportion to the total number of cells that colonize the surface. This leads us to model bacterial competition on a given particle, *n*, with a linear negative density-dependent growth function.

In this model, we assume that the bacterial growth on the particle is competitive in which the growth rate, μ_i is not constant but changes as a function of the total biomass on a particle. The negative density-dependent growth is modeled by assuming a linear function with the total particle associated cells ($B_{p,n} = \sum B_{p,n,i}$) on particle, *n*,

$$\begin{cases} \mu_i = \mu_{\max}\left(1 - \frac{B_{p,n}}{N_t}\right) \\ \mu_i = 0, \quad B_{p,n} > N_t \end{cases} \qquad (6)$$

Where $B_{p,n} = \sum B_{p,n,i}$, represents the total number of particle-attached cells, μ_i represents that growth rate of population *i*, μ_{max} indicates the maximal growth rate, in the absence of competition, and N_t represents the particle-specific carrying capacity. The net growth rate is assumed to be zero if more cells colonize a particle where bacteria have reached their carrying capacity; this occurs when bacteria have fully covered a particle's surface, such that the death or detachment of any cell is quickly replaced by the growth of another cell. The model assumes that free living cells cannot grow. We performed a sensitivity analysis to competitive growth kinetic parameterizations (maximum growth rate μ_{max} and carrying capacity, N_t) and showed that coexistence among bacterial detachment strategies is robust for a wide range of parameters (Figure 2 – Figure supplement 5).

Offspring production on the particle only occurs when particle associated cells accumulate a total biomass that is larger than the biomass of a single cell (m_d). For simplicity, we only measured biomass based on the dry mass of the cells. The biomass accumulation rate on a particle for population *i* is proportional to the available biomass on the particle, *n* and its exponential growth rate ($\frac{dB_{p,n,i}}{dt} = B_{p,n,i}\mu_i$). With this, the total number of offspring ($N_{o,i}$) on a particle for a time interval of, Δt can then be calculated as:

$$\begin{cases} N_{o,i} = \frac{B_{p,n,i}\mu_i}{m_d}\Delta t, & B_{p,n,i}\mu_i\Delta t > m_d \\ N_{o,i} = 0, \end{cases} \quad (7)$$

Particle-wide bacterial mortality

In the model, a general form of mortality on particles is considered that accounts for mortality induced by predation or particle sinking, taking cells beyond their preferred habitat. A constant fraction of particles (m_p) is randomly selected at each time interval (Δt) and their associated cells are removed from the particle. This fraction represents the particle-scale mortality rate (m_p). To maintain particle number equilibrium, a fraction m_p of uncolonized particles is introduced into the system and colonized by free-living populations ($B_{p,n,i}$=0).

Mortality of free-living cells is assumed to be caused by loss of biomass over a prolonged period of starvations from the absence of substrate uptake in the free-living phase. As described in Eq. 4, free-living cells (B_F) lose a constant fraction of their biomass (m_{Fi}) every time step as the cell maintenance. Note that though detachment of cells from a particle appears similar to mortality on particles, in the former, detached cells move to the free-living pool, while in the latter, cells die and do not add to either pool.

Particle degradation and turnover

We assume that a particle contains a finite amount of resources that is degraded by bacterial cells with a constant yield of converting the resources into biomass. From a previous study, we assume that the yield is about 5% and a significant fraction of particle degradation products are lost to the environment before being taken up by the cells[17].

Optimal residence time from optimal foraging theory

Optimal foraging theory describes the dispersal behavior of microbial populations in patchy environments assuming maximized growth return using the marginal value theorem. According to optimal foraging theory, the growth return of particle-associated bacteria is maximized if a bacterial cell detaches from the particle when its time-averaged uptake rate reaches its instantaneous uptake rate. We applied this assumption to obtain the optimal residence time on particles by tracking individual cells in our model and numerically calculating their instantaneous

uptake rate ($u(t)$) on a particle from the attachment time (t_a) to detachment using our population-based model. The residence time (t_r) is considered optimal when the following equation is satisfied[13]:

$$u(t_r) = \int_{t_a}^{t_r} \frac{u(t)dt}{(\tau_s + (t_r(\tau_s) - t_a))} \quad (8)$$

where τ_s is the search time and a function of the number of particles in the system. We calculated the search time from Eq.5 when the probability of the cell and particle encounter is above 95% (Figure 1 – Figure supplement 1).

Acknowledgements

This work was supported by Simons Foundation: Principles of Microbial Ecosystems (PriME) award number 542395. A.E. acknowledges funding from Swiss National Science Foundation: Grants P2EZP2 175128 and P400PB_186751. A.G. acknowledges support from the Gordon and Betty Moore Foundation as a Physics of Living Systems Fellow through award number GBMF4513.

Figures

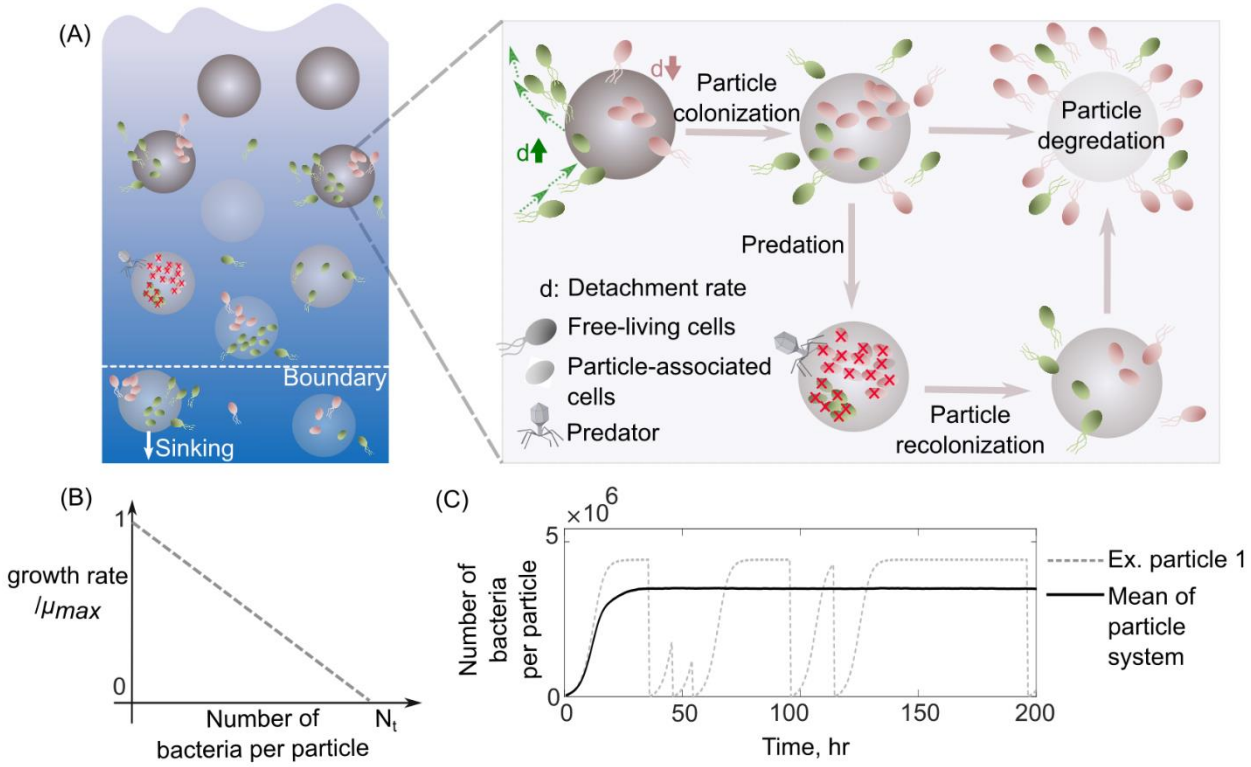

Figure 1: Schematic representation of the mathematical model simulating slow and fast dispersal strategies of bacterial populations that colonize particulate organic matter (A). The model assumes that the predation on a particle or sinking out of system's boundaries kills it's all associated populations. After infection, the non-colonized particle is then recolonized by free-living populations. As resources on a particle are consumed, its associated populations are dispersed and are added to the free-living populations. In this case, the old particle is replaced by a new un-colonized particle in the system. (B) The growth kinetics on a single particle is assumed to be density-dependent and decreases linearly as a function of the number of cells colonizing the particle. N_t represents the carrying capacity of the particle. C) The dynamics of particle-associated cells and their corresponding growth rates are shown for a system with 1000 particles. The mean values over many particles and an example of dynamics on a single particle are illustrated.

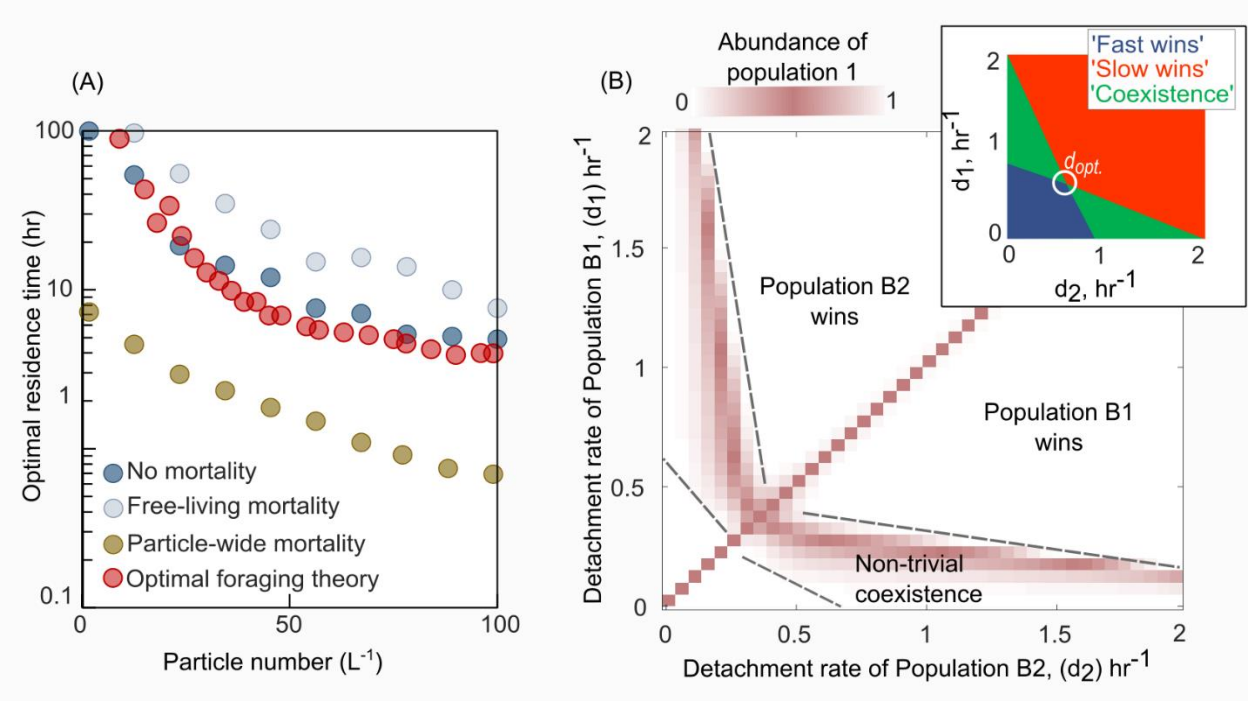

Figure 2. Variation in bacterial detachment strategies allow coexistence in the particle system. (A) Optimal residence time predicted by the population-based model and optimal foraging theory (Methods). Three scenarios with various particle-wide mortality (m_p) and mortality on free living populations (m_F) are simulated with the following rates: (i) particle-wide mortality (m_p= 0.05 hr^{-1}, m_F= 0.02 hr^{-1}), (ii) free living mortality (m_p= 0 hr^{-1}, m_F= 0.05 hr^{-1}) (iii) no mortality (m_p= 0 hr^{-1}, m_F= 0 hr^{-1}. To calculate optimal residence time based on optimal foraging theory (OFT), we used our model and tracked individual cells attaching to a particle. The time-averaged uptake rate of the attached cell and its instantaneous uptake rate were calculated. The residence time with similar instantaneous and time-averaged uptake rates is assumed to be optimal residence time based on OFT (see method for details). In our population-based model, the optimal residence time is assumed to be a residence time that maximizes the growth return from the particles. (B) The relative abundance of population one is shown for competition experiments of two populations with different detachment rates. The relative abundance is measured at the equilibrium, where no changes in the sizes of both populations are observed. The area with white color represents the conditions where either one of the populations is extinct. The mortally on particles is assumed 0.02hr^{-1}. (inset) Phase diagram of the coexistence as a function of detachment rates for two competing populations. $d_{opt.}$ represents the optimal detachment rate that the coexistence range nears zero. (B) The attachment rates are kept constant at 0.0005hr^{-1}. The number of particles is assumed to be 60 L^{-1}. The carrying capacity of

the particle is assumed to be $5e10^6$. Simulations are performed using our population-based mathematical model.

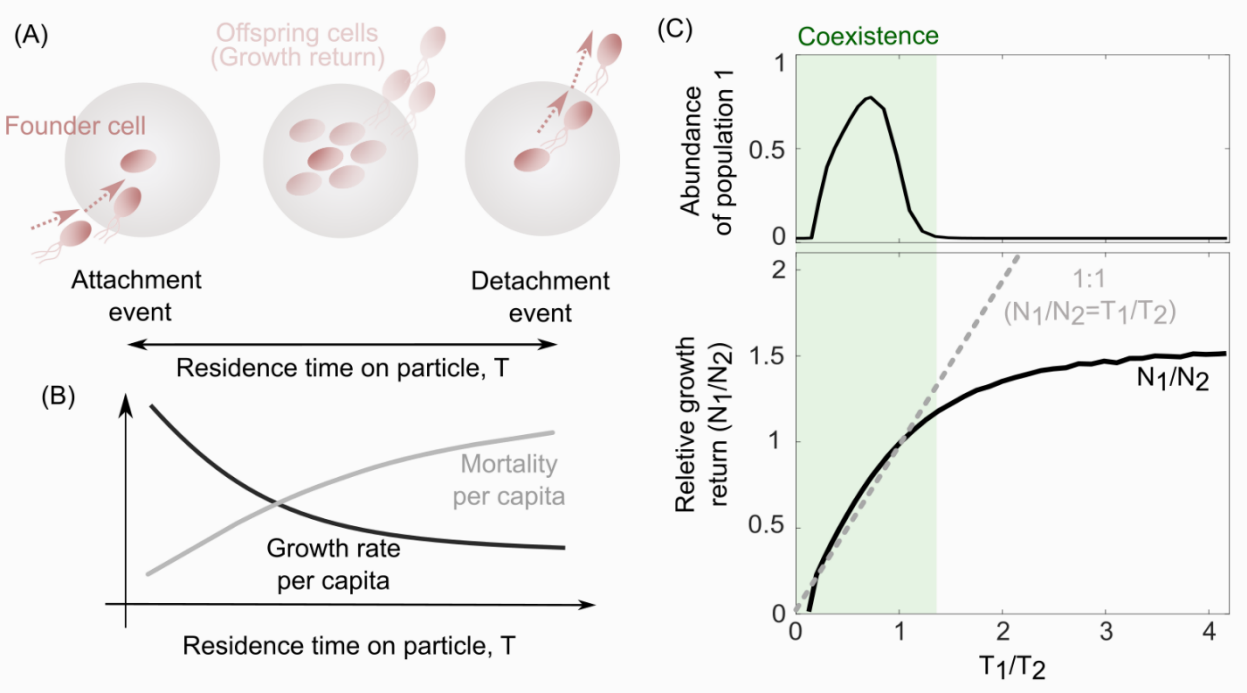

Figure 3. The trade-off between bacterial growth return and survival on the particles determine the coexistence range of competing populations. (A) The growth return of a single cell on a particle is calculated based on the number of offsprings produced during a single attachment/detachment event. (B) The growth rate on particles slows down as the particle is populated by offspring cells or new attaching cells that limit the net growth return from a particle. (C) The ratio of growth returns and survival of population one to population two per capita as a function of their radios of residence times is shown. The residence time on the particle is assumed to be the inverse of each population's detachment rate. The relative abundance of population one is shown for its corresponding simulations. The data are shown for the simulations where detachment rate of population 2 was kept constant at 0.2 hr^{-1}. Constant residence time for the population two (4hr) is considered while varying the residence time of the first population across simulations. 1:1 line represents a coarse-grained model for the coexistence criteria of two competing populations.

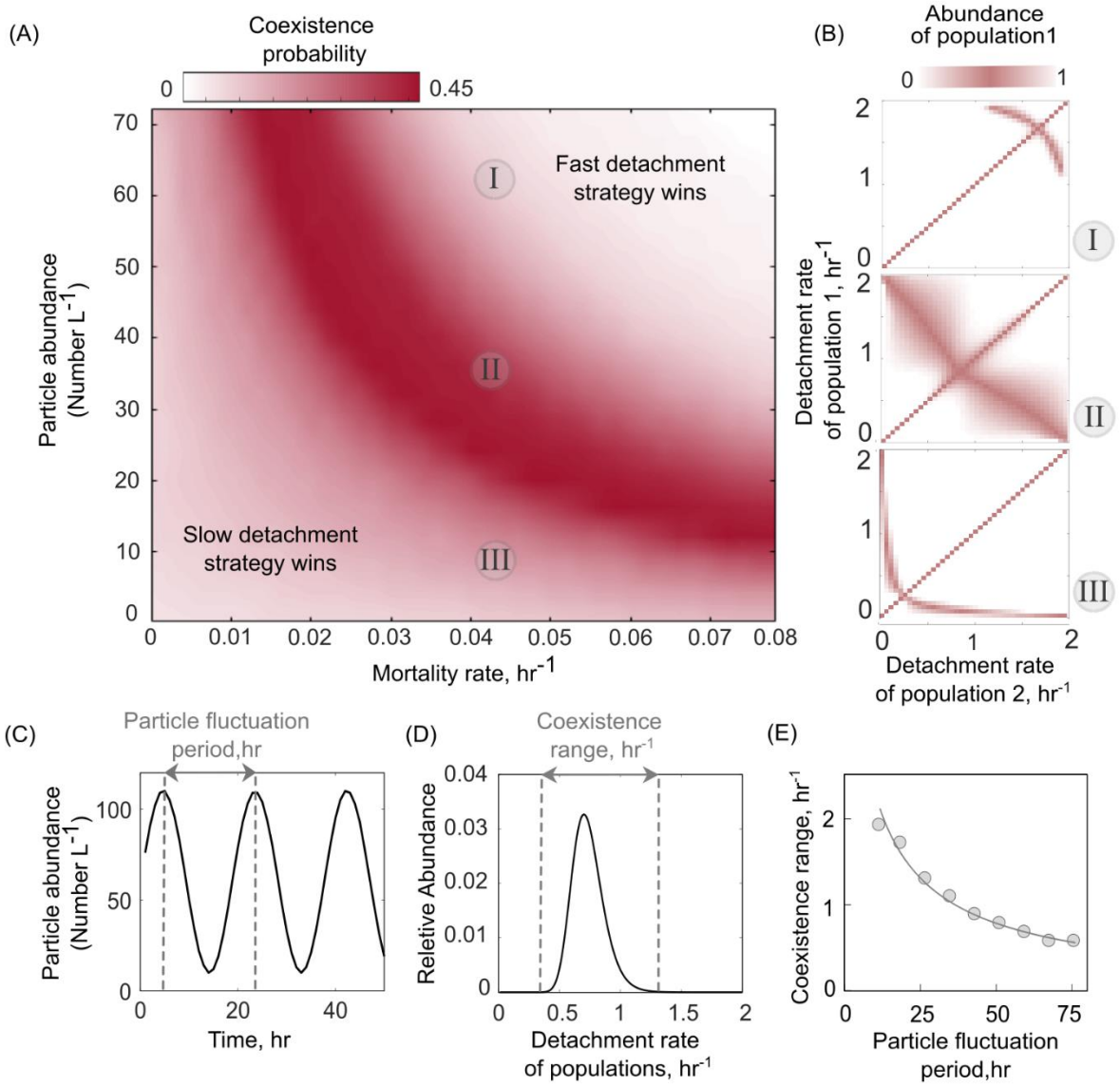

528

529 **Figure 4. Particle abundance and predation rate shape the coexistence of populations**
530 **with different dispersal strategies on the particle system**. (A) The coexistence probability is
531 shown for a range of particle abundances and predation rates. The coexistence probability is
532 calculated by performing multiple competition experiments across populations with various
533 detachment rates and quantifying the number of conditions that the coexistence between two
534 populations is found. (B) For three particle abundances in Figure 4A, the relative abundance of
535 population one is shown in competition experiments of two populations. The numbers in circles
536 refer to conditions in Figure 4A. Simulations are assumed to be at the equilibrium when no
537 changes in the size of either population are observed. The area with white color represents the
538 conditions where either one of the populations is extinct. (C) A sine function is introduced to

represent particle abundance fluctuations. (D) The coexistence range represents a range of detachment rates for populations that coexist at the equilibrium. Populations with relative abundances less than 5% of the most abundant population is assumed extinct. (E) The coexistence range is shown as a function of particle fluctuation period. The attachment rate and mortality rates are assumed to be ~0.0005hr^{-1} and ~0.045 hr^{-1}.

References

1. Azam, F. & Malfatti, F. Microbial structuring of marine ecosystems. *Nat. Rev. Microbiol.* **5**, 782–791 (2007).
2. Young, I. M. & Crawford, J. W. Interactions and self-organization in the soil-microbe complex. *Science* **304**, 1634–1637 (2004).
3. Ghilarov, A. M. The Paradox of the Plankton Reconsidered; Or, Why Do Species Coexist? *Oikos* (1984). doi:10.2307/3544244
4. Shoresh, N., Hegreness, M. & Kishony, R. Evolution exacerbates the paradox of the plankton. *Proc. Natl. Acad. Sci. U. S. A.* (2008). doi:10.1073/pnas.0803032105
5. Hutchinson, G. E. The Paradox of the Plankton. *Am. Nat.* (1961). doi:10.1086/282171
6. Goyal, A. & Maslov, S. Diversity, Stability, and Reproducibility in Stochastically Assembled Microbial Ecosystems. *Phys. Rev. Lett.* **120**, 158102 (2018).
7. Rodriguez-Valera, F. *et al.* Explaining microbial population genomics through phage predation. *Nat. Rev. Microbiol.* (2009). doi:10.1038/nrmicro2235
8. Muscarella, M. E., Boot, C. M., Broeckling, C. D. & Lennon, J. T. Resource heterogeneity structures aquatic bacterial communities. *ISME J.* (2019). doi:10.1038/s41396-019-0427-7
9. Saleem, M., Fetzer, I., Harms, H. & Chatzinotas, A. Diversity of protists and bacteria determines predation performance and stability. *ISME J.* (2013). doi:10.1038/ismej.2013.95
10. Milici, M. *et al.* Diversity and community composition of particle-associated and free-living bacteria in mesopelagic and bathypelagic Southern Ocean water masses: Evidence of dispersal limitation in the Bransfield Strait. *Limnol. Oceanogr.* (2017). doi:10.1002/lno.10487
11. Ganesh, S., Parris, D. J., Delong, E. F. & Stewart, F. J. Metagenomic analysis of size-fractionated picoplankton in a marine oxygen minimum zone. *ISME J.* (2014). doi:10.1038/ismej.2013.144
12. Crespo, B. G., Pommier, T., Fernández-Gómez, B. & Pedrós-Alió, C. Taxonomic composition of the particle-attached and free-living bacterial assemblages in the Northwest Mediterranean Sea analyzed by pyrosequencing of the 16S rRNA. *Microbiologyopen* (2013). doi:10.1002/mbo3.92
13. Yawata, Y., Carrara, F., Menolascina, F. & Stocker, R. Constrained optimal foraging by

marine bacterioplankton on particulate organic matter. *Proc. Natl. Acad. Sci.* (2020). doi:10.1073/pnas.2012443117

14. Fernandez, V. I., Yawata, Y. & Stocker, R. A Foraging Mandala for Aquatic Microorganisms. *ISME Journal* (2019). doi:10.1038/s41396-018-0309-4

15. Grossart, H. P., Kiørboe, T., Tang, K. & Ploug, H. Bacterial colonization of particles: Growth and interactions. *Appl. Environ. Microbiol.* (2003). doi:10.1128/AEM.69.6.3500-3509.2003

16. Yawata, Y. *et al.* Competition–dispersal tradeoff ecologically differentiates recently speciated marine bacterioplankton populations. *Proc. Natl. Acad. Sci.* **111**, 5622–5627 (2014).

17. Ebrahimi, A., Schwartzman, J. & Cordero, O. X. Cooperation and spatial self-organization determine rate and efficiency of particulate organic matter degradation in marine bacteria. *Proc. Natl. Acad. Sci. U. S. A.* (2019). doi:10.1073/pnas.1908512116

18. Boeuf, D. *et al.* Biological composition and microbial dynamics of sinking particulate organic matter at abyssal depths in the oligotrophic open ocean. *Proc. Natl. Acad. Sci. U. S. A.* (2019). doi:10.1073/pnas.1903080116

19. Dupont, C. L. *et al.* Genomes and gene expression across light and productivity gradients in eastern subtropical Pacific microbial communities. *ISME J.* (2015). doi:10.1038/ismej.2014.198

20. López-Pérez, M., Kimes, N. E., Haro-Moreno, J. M. & Rodriguez-Valera, F. Not all particles are equal: The selective enrichment of particle-associated bacteria from the mediterranean sea. *Front. Microbiol.* (2016). doi:10.3389/fmicb.2016.00996

21. Proctor, L. M. & Fuhrman, J. A. Roles of viral infection in organic particle flux. *Mar. Ecol. Prog. Ser.* (1991). doi:10.3354/meps069133

22. Weinbauer, M. G. *et al.* Viral ecology of organic and inorganic particles in aquatic systems: Avenues for further research. *Aquat. Microb. Ecol.* (2009). doi:10.3354/ame01363

23. Leventhal, G. E., Ackermann, M. & Schiessl, K. T. Why microbes secrete molecules to modify their environment: The case of iron-chelating siderophores. *J. R. Soc. Interface* (2019). doi:10.1098/rsif.2018.0674

24. Frazier, Z. & Alber, F. A computational approach to increase time scales in brownian dynamics-based reaction-diffusion modeling. *J. Comput. Biol.* (2012). doi:10.1089/cmb.2012.0027

25. Charnov, E. L. Optimal foraging, the marginal value theorem. *Theor. Popul. Biol.* (1976).

615 doi:10.1016/0040-5809(76)90040-X
616 26. Levin, S. A. & Paine, R. T. Disturbance, patch formation, and community structure. *Proc.*
617 *Natl. Acad. Sci. U. S. A.* (1974). doi:10.1073/pnas.71.7.2744
618 27. Kneitel, J. M. & Chase, J. M. Trade-offs in community ecology: Linking spatial scales and
619 species coexistence. *Ecology Letters* (2004). doi:10.1046/j.1461-0248.2003.00551.x
620 28. Tilman, D. Competition and biodiversity in spatially structured habitats. *Ecology* (1994).
621 doi:10.2307/1939377
622 29. Amarasekare, P. Competitive coexistence in spatially structured environments: A
623 synthesis. *Ecology Letters* (2003). doi:10.1046/j.1461-0248.2003.00530.x
624 30. Nilsson, E. *et al.* Genomic and Seasonal Variations among Aquatic Phages Infecting the
625 Baltic Sea Gammaproteobacterium Rheinheimera sp. Strain BAL341. *Appl. Environ.*
626 *Microbiol.* **85**, e01003-19 (2019).
627 31. Garin-Fernandez, A., Pereira-Flores, E., Glöckner, F. O. & Wichels, A. The North Sea
628 goes viral: Occurrence and distribution of North Sea bacteriophages. *Mar. Genomics* **41**,
629 31–41 (2018).
630 32. Luo, E., Aylward, F. O., Mende, D. R. & Delong, E. F. Bacteriophage distributions and
631 temporal variability in the ocean's interior. *MBio* **8**, (2017).
632 33. Lampitt, R. S., Hillier, W. R. & Challenor, P. G. Seasonal and diel variation in the open
633 ocean concentration of marine snow aggregates. *Nature* (1993). doi:10.1038/362737a0
634 34. Eckburg, P. B. *et al.* Microbiology: Diversity of the human intestinal microbial flora.
635 *Science (80-.).* (2005). doi:10.1126/science.1110591
636 35. Zhang, Z. *et al.* Spatial heterogeneity and co-occurrence patterns of human mucosal-
637 associated intestinal microbiota. *ISME J.* (2014). doi:10.1038/ismej.2013.185
638 36. Young, I. M. & Crawford, J. W. Interactions and self-organization in the soil-microbe
639 complex. *Science* (2004). doi:10.1126/science.1097394
640 37. Holmfeldt, K., Middelboe, M., Nybroe, O. & Riemann, L. Large variabilities in host strain
641 susceptibility and phage host range govern interactions between lytic marine phages and
642 their Flavobacterium hosts. *Appl. Environ. Microbiol.* (2007). doi:10.1128/AEM.01399-07
643 38. Roux, S. *et al.* Assessing the diversity and specificity of two freshwater viral communities
644 through metagenomics. *PLoS One* (2012). doi:10.1371/journal.pone.0033641
645 39. Suttle, C. A. & Chan, A. M. Dynamics and distribution of cyanophages and their effect on
646 marine Synechococcus spp. *Appl. Environ. Microbiol.* (1994).
647 doi:10.1128/aem.60.9.3167-3174.1994
648 40. Suttle, C. A. Viruses in the sea. *Nature* (2005). doi:10.1038/nature04160

41. Taylor, J. R. & Stocker, R. Trade-offs of chemotactic foraging in turbulent water. *Science (80-.).* **338**, 675–679 (2012).
42. Vetter, Y. A., Deming, J. W., Jumars, P. A. & Krieger-Brockett, B. B. A predictive model of bacterial foraging by means of freely released extracellular enzymes. *Microb. Ecol.* (1998). doi:10.1007/s002489900095
43. Newman, J. A. Patch Use under Predation Hazard: Foraging behavior in a Simple Stochastic Environment. *Oikos* **61**, 29–44 (1991).
44. Abrams, P. A. Optimal traits when there are several costs: the interaction of mortality and energy costs in determining foraging behavior. *Behav. Ecol.* **4**, 246–259 (1993).
45. Litchman, E. Competition and coexistence of phytoplankton under fluctuating light: Experiments with two cyanobacteria. *Aquat. Microb. Ecol.* (2003). doi:10.3354/ame031241
46. Li, L. & Chesson, P. The effects of dynamical rates on species coexistence in a variable environment: The paradox of the plankton revisited. *Am. Nat.* (2016). doi:10.1086/687111
47. Catorci, A., Piermarteri, K., Penksza, K., Házi, J. & Tardella, F. M. Filtering effect of temporal niche fluctuation and amplitude of environmental variations on the trait-related flowering patterns: Lesson from sub-Mediterranean grasslands. *Sci. Rep.* (2017). doi:10.1038/s41598-017-12226-5
48. Sousa, W. P. Disturbance in Marine Intertidal Boulder Fields: The Nonequilibrium Maintenance of Species Diversity. *Ecology* (1979). doi:10.2307/1936969
49. Teeling, H. *et al.* Substrate-controlled succession of marine bacterioplankton populations induced by a phytoplankton bloom. *Science (80-.).* (2012). doi:10.1126/science.1218344
50. West, N. J., Obernosterer, I., Zemb, O. & Lebaron, P. Major differences of bacterial diversity and activity inside and outside of a natural iron-fertilized phytoplankton bloom in the Southern Ocean. *Environ. Microbiol.* (2008). doi:10.1111/j.1462-2920.2007.01497.x
51. Wemheuer, B. *et al.* Impact of a phytoplankton bloom on the diversity of the active bacterial community in the southern North Sea as revealed by metatranscriptomic approaches. *FEMS Microbiol. Ecol.* (2014). doi:10.1111/1574-6941.12230
52. Datta, M. S., Sliwerska, E., Gore, J., Polz, M. & Cordero, O. X. Microbial interactions lead to rapid micro-scale successions on model marine particles. *Nat. Commun.* **7**, 11965 (2016).
53. Dal Bello, M., Lee, H., Goyal, A. & Gore, J. Resource–diversity relationships in bacterial communities reflect the network structure of microbial metabolism. *Nat. Ecol. Evol.* **5**, 1424–1434 (2021).

54. Lauro, F. M. *et al.* The genomic basis of trophic strategy in marine bacteria. *Proc. Natl. Acad. Sci.* **106**, 15527 LP – 15533 (2009).
55. Pascual-García, A. *et al.* Turnover in life-strategies recapitulates marine microbial succession colonizing model particles. (2021). doi:10.1101/2021.11.05.466518
56. Taylor, J. R. & Stocker, R. Trade-offs of chemotactic foraging in turbulent water. *Science (80-.).* (2012). doi:10.1126/science.1219417
57. Son, K., Menolascina, F. & Stocker, R. Speed-dependent chemotactic precision in marine bacteria. *Proc. Natl. Acad. Sci. U. S. A.* 1–6 (2016). doi:10.1073/pnas.1602307113
58. Stocker, R., Seymour, J. R., Samadani, A., Hunt, D. E. & Polz, M. F. Rapid chemotactic response enables marine bacteria to exploit ephemeral microscale nutrient patches. *Proc. Natl. Acad. Sci.* (2008). doi:10.1073/pnas.0709765105

Supplementary Figure Legends

Figure 1 – Figure supplement 1. (A) Encounter probability of a bacterial cell and a particle as a function of cell-particle distance, $D_{c,p}$. An analytical model based on the hitting probability of two objects from random walk theory is used to obtain the encounter probability (Eq. 5). Bacterial cell and particle sizes are assumed to be 1 and 100μm, respectively. Simulations are performed for two time-intervals of 1 and 10 seconds. (B) The rate of free living bacterial cells attachment to particles as a function of time for various number particle availability in the environment.

Figure 2 – Figure supplement 1. Two examples of population dynamics are shown wherein both populations reach a stable coexistence (I), while in the other scenario (II), one population is extinct. The detachment rates of the populations B1 and B2 in scenarios I and II are (0.7hr-1, 0.2hr-1) and (0.7hr-1, 1hr-1), respectively. These population dynamics correspond to the conditions simulated in Figure 2A.

Figure 2 – Figure supplement 2. The relative abundance of population one is shown when no mortality on particles is considered for competition experiments of two populations with different detachment rates. The parameters for the simulations are selected similar to Figure 2A, except with no particle-wide mortality.

Figure 2 – Figure supplement 3. In the absence of environmental fluctuations, competition experiment between populations with different detachment rates shows an emergence of an optimal detachment strategy that outcompete other populations. The relative abundances of populations with different detachment rates are shown over time. The simulations start with 100 populations with the same relative abundances that they only differ in their detachment rates. In this simulation, bacterial cells colonize 1000 particles with a constant attachment rate (~0.0005hr-1). Two mortality rates are simulated (low: 0.04hr-1 and high 0.08hr-1)

Figure 2 – Figure supplement 4. Cooperative growth kinetics restricts the coexistence range among two populations with different dispersal strategies. (A) Schematic representation of various growth kinetics on particles as a function of the number of bacteria on particles. (B) The coexistence range among two populations is shown as a function of the detachment rate of the second population. The coexistence range represents a range of detachment rates for both

populations that coexist at the equilibrium. Inset panel represents the relative abundance of population 1 for different detachment rates. Detachment rates with relative abundances less than 5% is assumed extinct. The mortally on particles is assumed 0.02hr-1. The attachment rates are kept constant at 0.0005hr-1. The number of particles is assumed to be 60L-1. The carrying capacity and maximum growth rates are assumed, Nt=5×106 and μmax = 0.50 hr-1, respectively.

Figure 2 – Figure supplement 5. The sensitivity of coexistence among bacterial detachment strategies to competitive growth kinetic parameterizations (Eq. 6: maximum growth rate μmax and carrying capacity, Nt). The relative abundance of population one is shown for competition experiments of two populations with different detachment rates and for two different values of maximum growth rates and carrying capacities. The area with white color represents the conditions where either one of the populations is extinct. The mortally on particles is assumed 0.02hr-1. The attachment rates are kept constant at 0.0005hr-1. The number of particles is assumed to be 60L-1.

Figure 4 – Figure supplement 1. Particle abundance distributions extracted from the field observations. The particle abundances are extracted over many field observations across many aquatic environments at different geographical locations (Möller et al. 2012; Ashijan et al., 2005; Gallager et al., 2004; Norrbin et al., 1996). The mean particle abundance over these field data is approximately 25 per liter.

Figure 4 – Figure supplement 2. The durations of environmental fluctuation periods for particle abundances are extracted from field data33. (A) The fluctuations in particle abundance are characterized by quantifying fluctuation periods from the time difference between two neighboring local minimum and maximum, as illustrated in the schematic. (B) Probability distribution functions for fluctuation periods in particle abundances obtained from field observations.

Supplementary Figures

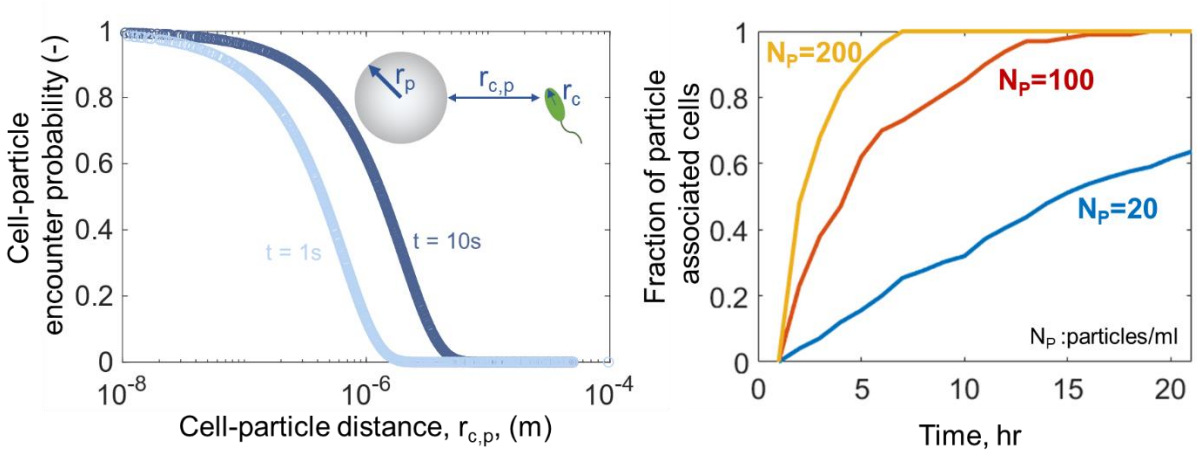

Figure 1 – Figure supplement 1. (A) Encounter probability of a bacterial cell and a particle as a function of cell-particle distance, $D_{c,p}$. An analytical model based on the hitting probability of two objects from random walk theory is used to obtain the encounter probability (Eq. 5). Bacterial cell and particle sizes are assumed to be 1 and 100μm, respectively. Simulations are performed for two time-intervals of 1 and 10 seconds. (B) The rate of free living bacterial cells attachment to particles as a function of time for various number particle availability in the environment.

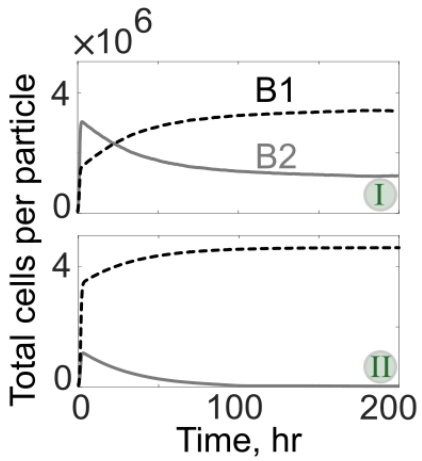

Figure 2 – Figure supplement 1. Two examples of population dynamics are shown wherein both populations reach a stable coexistence (I), while in the other scenario (II), one population is extinct. The detachment rates of the populations B1 and B2 in scenarios I and II are ($0.7hr^{-1}$, $0.2hr^{-1}$) and ($0.7hr^{-1}$, $1hr^{-1}$), respectively. These population dynamics correspond to the conditions simulated in Figure 2A.

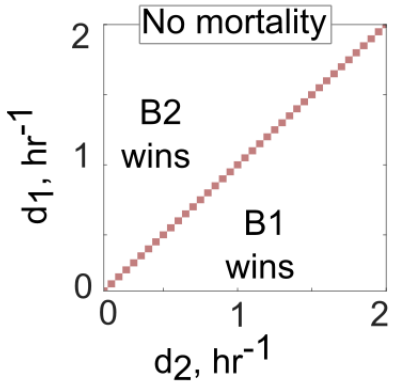

Figure 2 – Figure supplement 2. The relative abundance of population one is shown when no mortality on particles is considered for competition experiments of two populations with different detachment rates. The parameters for the simulations are selected similar to Figure 2A, except with no particle-wide mortality.

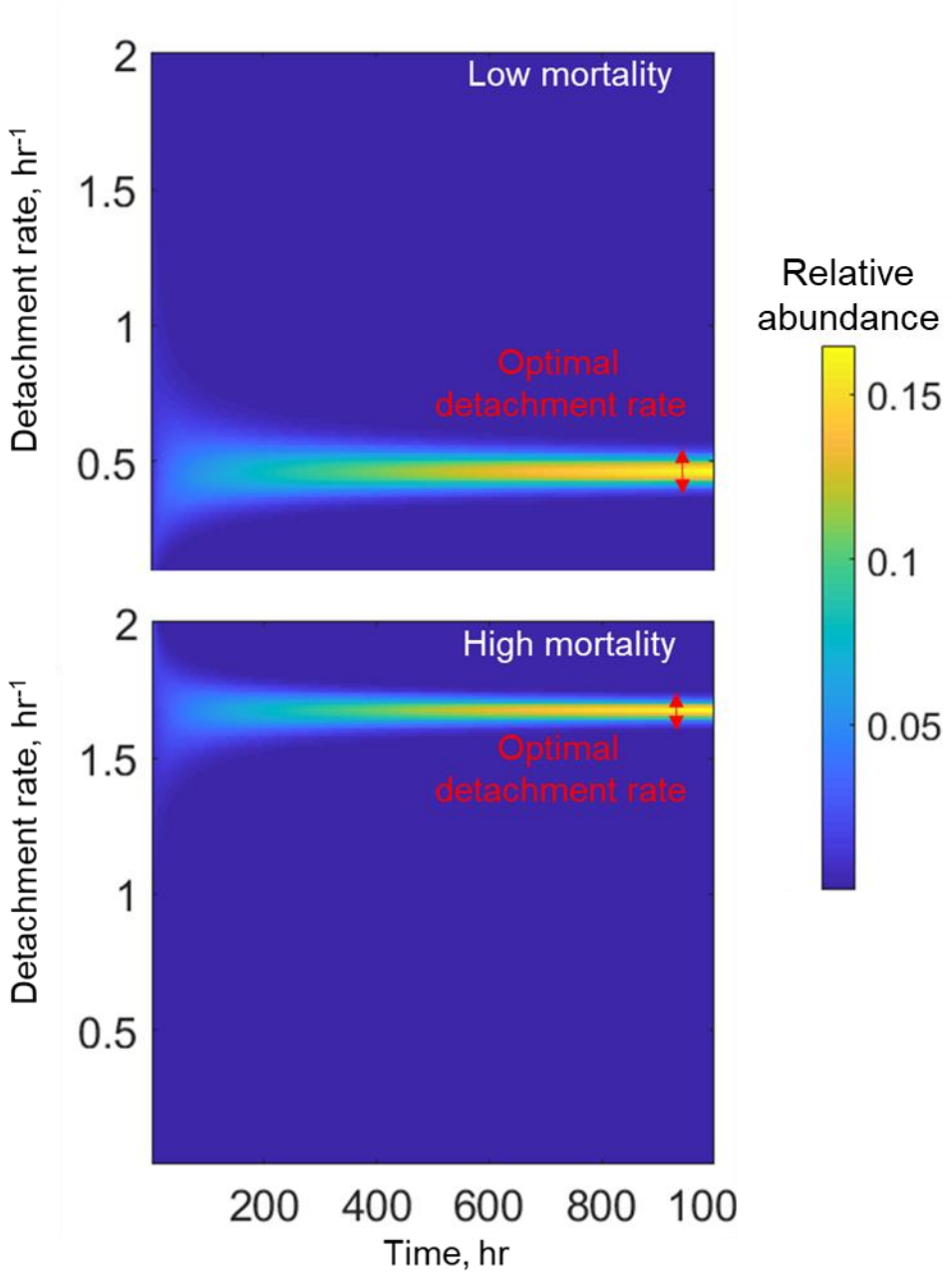

795
796

797 Figure 2 – Figure supplement 3. In the absence of environmental fluctuations, competition
798 experiment between populations with different detachment rates shows an emergence of an
799 optimal detachment strategy that outcompete other populations. The relative abundances of
800 populations with different detachment rates are shown over time. The simulations start with 100
801 populations with the same relative abundances that they only differ in their detachment rates. In
802 this simulation, bacterial cells colonize 1000 particles with a constant attachment rate
803 (~0.0005hr^{-1}). Two mortality rates are simulated (low: 0.04hr^{-1} and high 0.08hr^{-1})

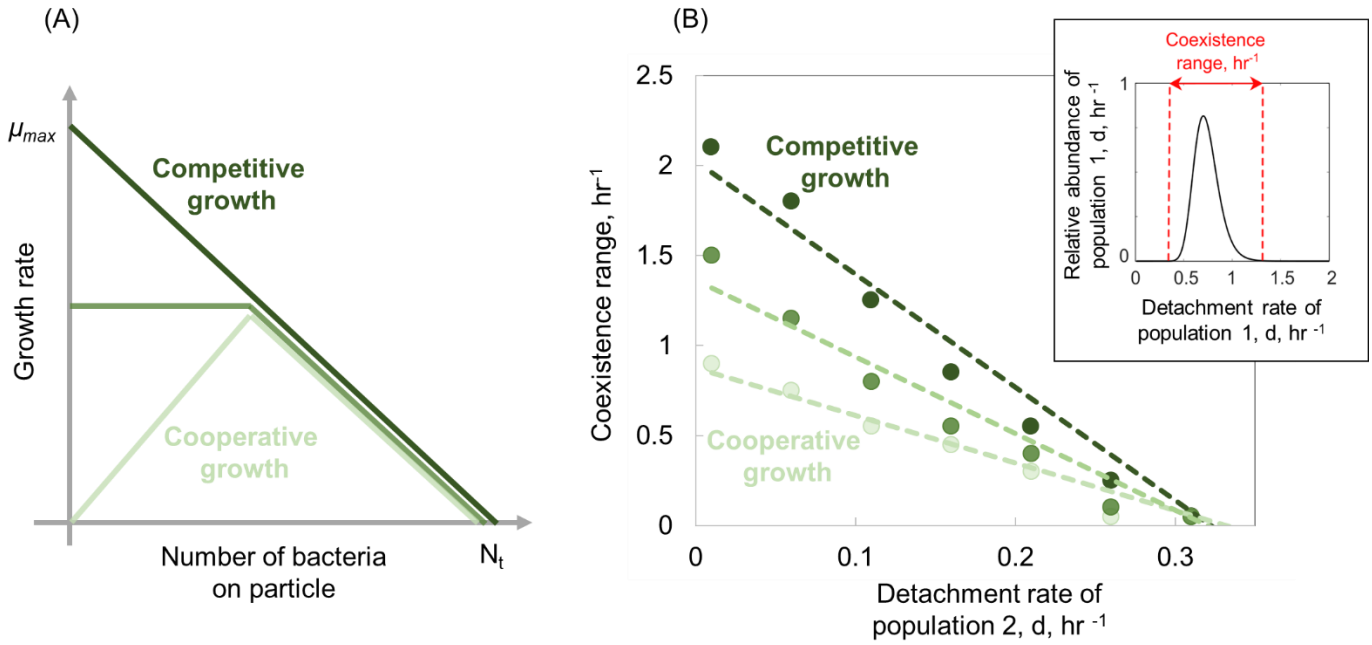

Figure 2 – Figure supplement 4. Cooperative growth kinetics restricts the coexistence range among two populations with different dispersal strategies. (A) Schematic representation of various growth kinetics on particles as a function of the number of bacteria on particles. (B) The coexistence range among two populations is shown as a function of the detachment rate of the second population. The coexistence range represents a range of detachment rates for both populations that coexist at the equilibrium. Inset panel represents the relative abundance of population 1 for different detachment rates. Detachment rates with relative abundances less than 5% is assumed extinct. The mortally on particles is assumed 0.02hr^{-1}. The attachment rates are kept constant at 0.0005hr^{-1}. The number of particles is assumed to be 60L^{-1}. The carrying capacity and maximum growth rates are assumed, N_t=5×10^6 and μ_{max} = 0.50 hr^{-1}, respectively.

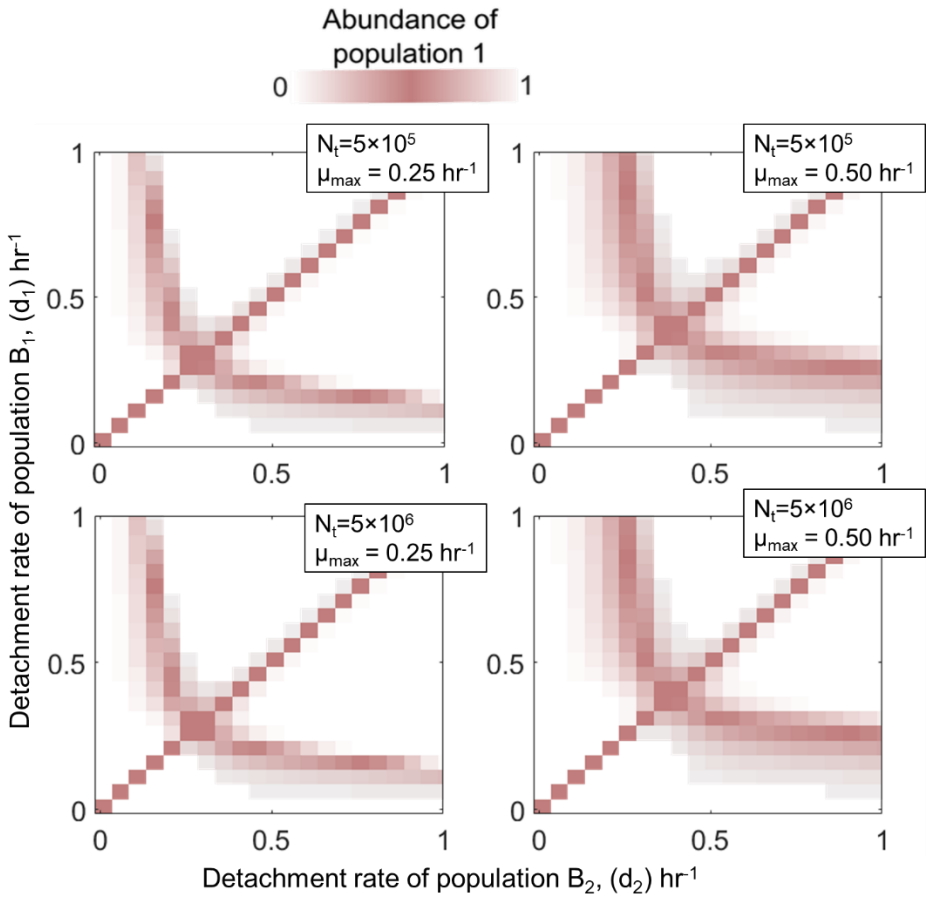

Figure 2 – Figure supplement 5. The sensitivity of coexistence among bacterial detachment strategies to competitive growth kinetic parameterizations (Eq. 6: maximum growth rate μ_{max} and carrying capacity, N_t). The relative abundance of population one is shown for competition experiments of two populations with different detachment rates and for two different values of maximum growth rates and carrying capacities. The area with white color represents the conditions where either one of the populations is extinct. The mortally on particles is assumed 0.02hr^{-1}. The attachment rates are kept constant at 0.0005hr^{-1}. The number of particles is assumed to be 60L^{-1}.

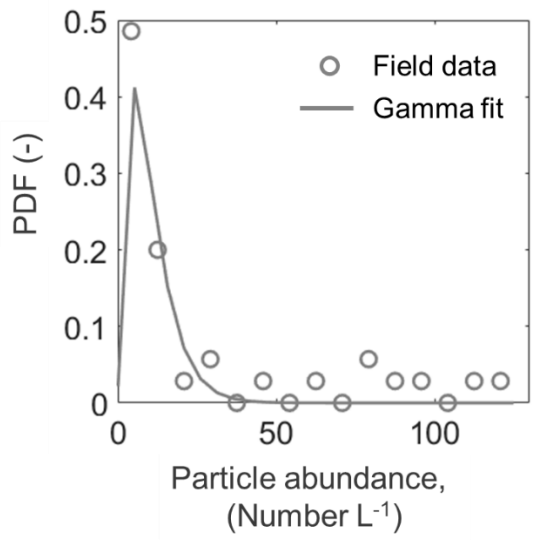

833
834
835 Figure 4 – Figure supplement 1. Particle abundance distributions extracted from the field
836 observations. The particle abundances are extracted over many field observations across many
837 aquatic environments at different geographical locations (Möller et al. 2012; Ashijan et al., 2005;
838 Gallager et al., 2004; Norrbin et al., 1996). The mean particle abundance over these field data is
839 approximately 25 per liter.
840

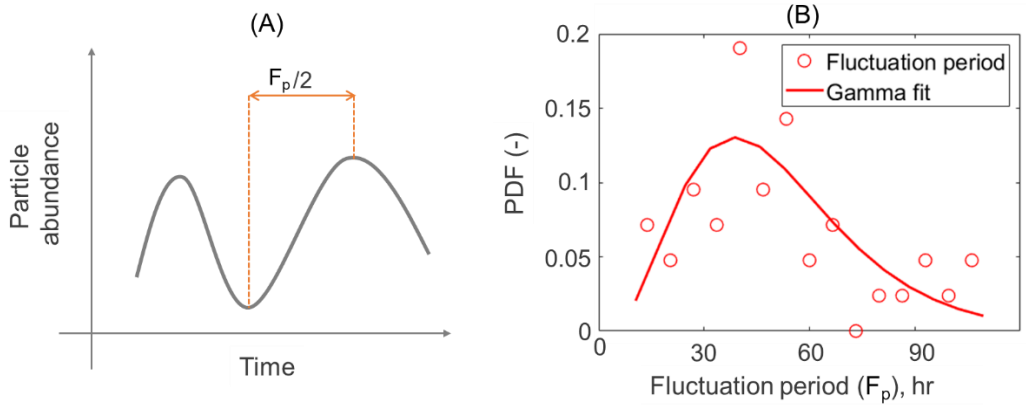

841
842
843 Figure 4 – Figure supplement 2. The durations of environmental fluctuation periods for particle
844 abundances are extracted from field data[33]. (A) The fluctuations in particle abundance are
845 characterized by quantifying fluctuation periods from the time difference between two
846 neighboring local minimum and maximum, as illustrated in the schematic. (B) Probability
847 distribution functions for fluctuation periods in particle abundances obtained from field
848 observations.